Chemistry and Physics of Lipids 220 (2019) 1–5

Contents lists available at ScienceDirect

Chemistry and Physics of Lipids

journal homepage: www.elsevier.com/locate/chemphyslip

Review

Nanodiscs bounded by styrene-maleic acid allow *trans-cis* isomerization of enclosed photoswitches of azobenzene labeled lipids

J.J. Domínguez Pardo*, C.A. van Walree, M.R. Egmond, M.C. Koorengevel, J.A. Killian*

Membrane Biochemistry & Biophysics, Bijvoet Center for Biomolecular Research, Department of Chemistry, Faculty of Science, Padualaan 8, 3584 CH, Utrecht, the Netherlands

ARTICLE INFO

Keywords:
SMA
Azobenzene
Nanodisc
Isomerization
Lipid packing
Lateral pressure

ABSTRACT

Styrene-and-maleic acid (SMA) copolymers behave as amphipathic belts encircling lipids in the form of nanodiscs. It is unclear to what extent the SMA belt affects the order and dynamics of the enclosed lipids. We aimed to obtain insight into this by making use of synthetic azobenzene-labeled phospholipids incorporated into di-16:0 PC nanodiscs. Azobenzene lipids undergo geometric isomerization upon exposure to light at 365 nm, resulting in the formation of *cis*-isomers that possess a larger cross-sectional area than the *trans*-isomers. The influence of the lipid properties on the kinetics and extent of isomerization of the azobenzene groups was first tested in large unilamellar vesicles constituted by lipid mixtures with different packing properties of the acyl chains. Fastest isomerization kinetics were found when azolipids were present in membranes supplemented with lysolipids and slowest in those supplemented with di-unsaturated lipids, suggesting that the isomerization rate is sensitive to the lateral pressure profile in the lipid bilayer and hence may be considered a convenient tool to monitor packing properties of lipids enclosed in nanodiscs. When azolipids were incorporated in SMA-bounded nanodiscs, azolipid isomerization was found to take place readily, indicating that SMA polymers behave as rather flexible belts and allow expansion of the enclosed lipid material.

1. Introduction

SMA (styrene-maleic acid) copolymers are in the spotlight of membrane protein research due to their ability to solubilize lipid membranes into nanodiscs (for reviews see e.g. (Dörr et al., 2016; Esmaili and Overduin, 2017; Stroud et al., 2018)). This allows membrane proteins to be isolated and studied in their native membrane environment (Dörr et al., 2014; Prabudiansyah et al., 2015; Swainsbury et al., 2014; Sun et al., 2018). However, it does not necessarily imply that proteins that are confined in such nanodiscs have the same motional freedom as in the native membrane. The nanodiscs are surrounded by a polymer belt with the styrene units intercalating between adjacent lipids (Dominguez Pardo et al., 2017; Grethen et al., 2017; Orwick et al., 2012; Jamshad et al., 2015; Xue et al., 2018), and it is possible that this belt affects the structure and organization of molecules that are enclosed in the nanodiscs.

Another potential factor of influence for the properties of enclosed molecules is the dynamic behavior of the nanodiscs. Already in an early stage in SMA research it was recognized that the tetrameric channel protein KscA can be transferred from nanodiscs to a lipid bilayer (Dörr et al., 2014). Since then, exchange of lipids has been reported between nanodiscs in solution (Grethen et al., 2018; Cuevas Arenas et al., 2017; Domínguez Pardo et al., 2018) and lipid monolayers (Hazell et al., 2016) and it was demonstrated that fast collisional lipid transfer between nanodiscs occurs, which was thought to arise from the flexible nature of the polymer belt. Very recently, also polymer exchange between nanodiscs has been reported (Schmidt and Sturgis, 2018).

To gain insight into the properties of molecules enclosed in SMA-bounded nanodiscs, a number of studies have been performed using lipid model membrane systems. However, from these studies it is not clear whether SMA has an ordering or a disordering effect on the enclosed lipids. EPR experiments using spin-labeled stearic acid (C11-label) in di-14:0 PC nanodiscs indicated an overall increase in order for C8—C12 while the adjacent methylene groups remained unperturbed (Orwick et al., 2012). On the other hand, TEMPO EPR (Orwick et al., 2012) and DSC analyses (Jamshad et al., 2015; Orwick et al., 2012; Grethen et al., 2017; Dominguez Pardo et al., 2017; Domínguez Pardo et al., 2018) on di-14:0 PC nanodiscs revealed a lowering of the melting phase transition temperature and a decrease in cooperativity between lipids participating in the gel-to-fluid phase transition, suggesting a

Abbreviations: LUV, large unilamellar vesicle; PC, phosphatidylcholine; SMA, copolymer, styrene- maleic acid copolymer; SMALP, styrene- maleic acid lipid particle

* Corresponding authors.
E-mail address: J.A.Killian@uu.nl (J.J. Domínguez Pardo).

https://doi.org/10.1016/j.chemphyslip.2019.02.002
Received 22 December 2018; Received in revised form 14 February 2019; Accepted 14 February 2019
Available online 16 February 2019

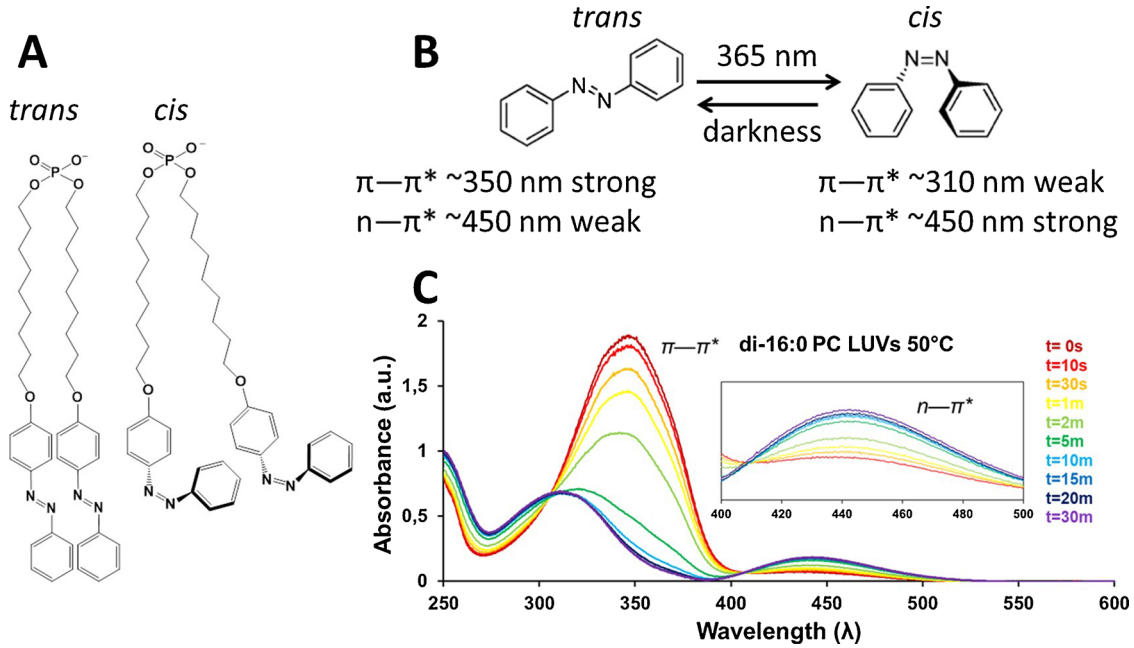

Fig. 1. A) Molecular structure of *trans*-Azo-9P and *cis*-Azo-9P. B) Schematic representation of the isomerization of azobenzene. C) Spectra obtained for di-16:0 PC/Azo-9P (9:1 M ratio) LUVs after light exposure at 350 nm. All experiments were conducted at 50 °C.

disordering effect.

Here, we aim to gain insight into the effect of the SMA belt on enclosed material by studying the behavior of synthetic di-{9-[(4-phenylazo)-phenoxy]-nonyl} phosphate (i.e. Azo-9 P, see forthcoming Fig. 1A) lipids in nanodiscs. The azobenzenes attached to these lipids undergo geometric isomerization upon exposure of light at 365 nm (for reviews see (Beharry and Woolley, 2011; Bandara and Burdette, 2012)) from an almost planar, extended *trans*-configuration to a non-planar, contracted *cis*-configuration with a larger cross-sectional area (Elbing et al., 2008; Nakayama et al., 1997). Whether isomerization of azobenzene in nanodiscs is hindered or not will depend on lipid packing and rigidity of the local environment. *Trans*-to-*cis* isomer conversion can be tracked by UV/Vis spectroscopy as a decrease in A_{350nm} and a small increase in A_{450nm}. We will illustrate that this approach in principle is feasible by demonstrating that isomerization of Azo-9 P in phosphatidylcholine vesicular self-assemblies is sensitive to the packing properties of the acyl chains of the surrounding lipids. Subsequently we will show that isomerization of Azo-9 P takes place efficiently in SMA-bounded nanodiscs. This supports the notion that nanodiscs consist of dynamic particles that “breathe” and thus allow the expansion of enclosed lipid and protein material. This dynamic behavior will be important for the suitability of using SMA-bounded nanodiscs for studying membrane proteins whose activity requires conformational changes that involve changes in molecular area.

2. Materials and methods

2.1. Materials

1,2-dipalmitoleoyl-sn-glycero-3-phosphocholine (di-16:0 PC), 1,2-dipalmitoleoyl-sn-glycero-3-phosphocholine (di-16:1 PC) and 1-oleoyl-2-hydroxy-sn-glycero-3-phosphocholine (lyso-18:1 PC) were purchased from Avanti Polar Lipids (Alabaster, AL, USA). Xiran 30010 (SMA 2:1, styrene-to-maleic anhydride molar ratio of 2:1) and Xiran 25010 (SMA 3:1, styrene-to-maleic anhydride molar ratio of 3:1) both with a weight average molecular weight of ˜10 kDa were obtained as a kind gift from Polyscope Polymers (Geleen, The Netherlands). The polymers were converted to the acid form by hydrolysis under base-catalytic conditions as detailed by Scheidelaar et al (Scheidelaar et al., 2015). 4-Phenylazophenol, 9-bromononan-1-ol and all other chemicals were purchased from Sigma-Aldrich (St. Louis, MO, USA).

2.2. Preparation of large unilamellar vesicles (LUVs)

Phospholipid stock solutions were prepared in chloroform/methanol (9:1, v/v) as 10 mM solutions based on the analysis of total phosphate (Rouser et al., 1970). Azo-9 P (Kuiper and Engberts, 2004; Kuiper et al., 2003) stock solutions were prepared identically but in methanol/chloroform (1:1, v/v). Aliquots from the phospholipid stock solutions and from the Azo-9 P stock solutions, if required, were mixed and the solvent was removed under a stream of N_2. The resulting lipid film was dried in a desiccator under vacuum for at least 1 h. Multilamellar vesicles (MLVs) were obtained by hydrating the lipid films with buffer (50 mM Tris-HCl, 150 mM NaCl, pH 8.0) to a final concentration of 10 mM. The samples were then subjected to 10 freeze-thaw cycles, each consisting of 3 min freezing in liquid N_2 and 3 min thawing in a water bath at 60 °C, well above T_m of the lipids (Lewis et al., 1987). Finally, the dispersions of MLVs were extruded at least 10 times through 200 nm polycarbonate filters (Avanti Polar Lipids, Alabaster, USA) at approximately ˜50 °C, above T_m of the lipids (Lewis et al., 1987).

2.3. Preparation of nanodiscs

700 μL aliquots of 10 mM dispersions of LUVs were diluted to 1 mM with solubilization buffer (Tris 50 mM, NaCl 150 mM, Tris-HCl pH = 8.0) and mixed with SMA to a final SMA-to-lipid mass ratio of 3.0. The mixture was incubated for at least 15 h above T_m of the lipids and under constant shaking. After solubilization, the samples were placed in an Optima Max ultracentrifuge (Beckman-Coulter, Brea, CA, USA). Traces of non-solubilized material were removed by centrifugation at 115,000 × *g* for 1 h at 4 °C. Phosphate determination (Rouser et al., 1970) showed that the phospholipid content in the nanodiscs was rather similar to that in the original LUVs. The concentration of azobenzene in nanodiscs was estimated from A_{350nm}, based on calibration with known concentrations of azobenzene in LUVs.

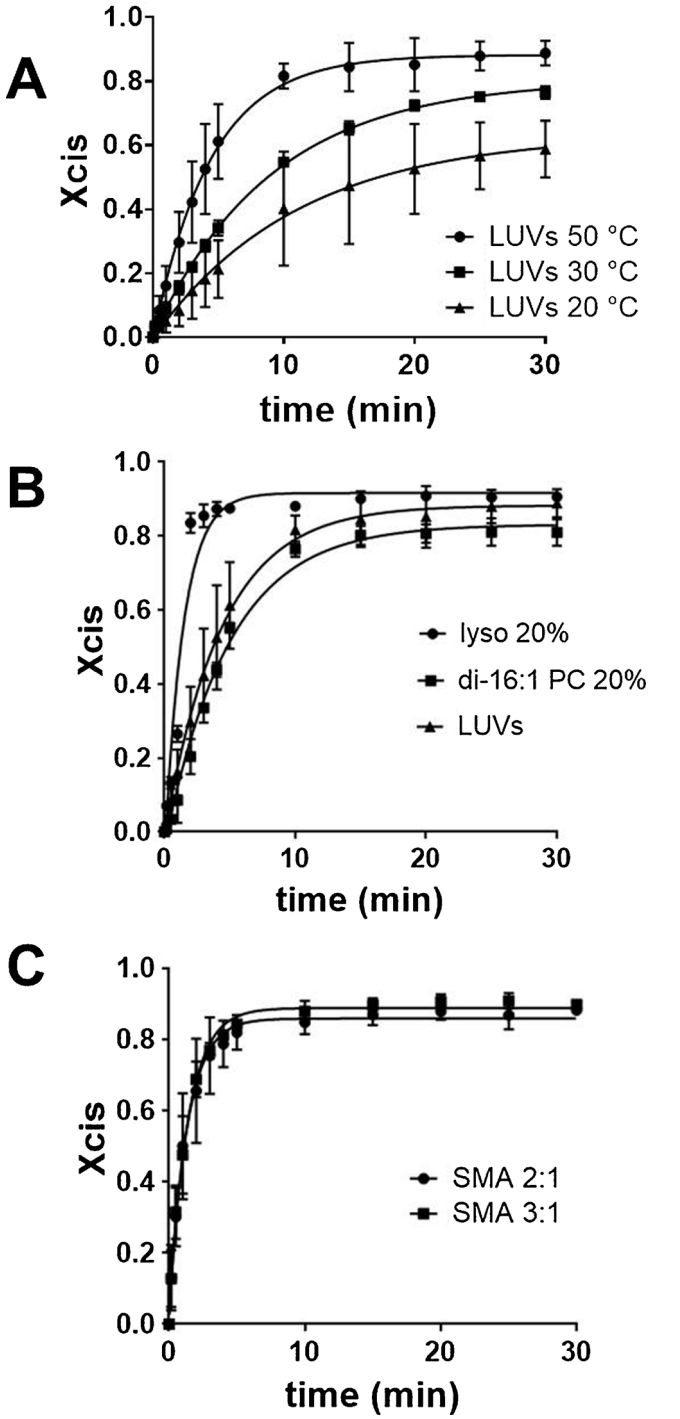

Fig. 2. Plot of *Xcis* (isomerization degree) with time (min) of *trans*-Azo-9P in di-16:0 PC at different temperatures (A), in LUVs of different lipid composition at 50 °C (B), and in di-16:0 PC SMA-bounded nanodiscs at 50 °C (C). *Xcis* is defined as 1-$[A_{350}]_t/[A_{350}]_0$. Error bars represent the standard error of at least 2 independent experiments. Data was fitted to equation 2 by using GraphPad Prism™.

2.4. Isomerization of Azo-9P

The *trans*-to-*cis* isomerization of Azo-9P was conducted using a SPF-500C spectrofluorimeter (SLM Instruments, NY). The quartz cuvette containing the nanodisc solutions or LUV dispersions from the UV-Vis assay was placed in the cuvette holder at the desired temperature and excited at 365 nm for different time periods in the range of 10 s to 120 m (power 250 W).

2.5. UV–vis spectroscopy

UV-Vis scans were performed using a Lambda 18 spectrophotometer (PerkinElmer, Waltham, MA). Briefly, 700 µL aliquots of 1 mM nanodisc solutions or LUVs dispersions were transferred to a quartz cuvette and equilibrated at the desired temperature for 1 min with a cell Peltier element. Scans were recorded in the range of 200 nm–600 nm at a speed of 240 nm/min. All samples were blanked against identical self-assemblies but without Azo-9 P. Data points were obtained every 0.25 s.

2.6. Synthesis of Azo-9P

The synthesis of Azo-9P was conducted as detailed by Kuiper et al., 2003 (Kuiper et al., 2003). ^{1}H NMR (300 MHz, CD_3OD 1:1 v/v): δ = 1.24–1.46 (m, 20 H), 1.59–2.02 (m, 8 H), 3.81 (t, 4 H), 4.02 (t, 4 H), 6.97–7.0 (d, J = 8.8 Hz, 4 H), 7.4–7.51 (m,6 H), 7.83–7.90 (m, 8 H). ^{13}C NMR (75 MHz, CD_3OD 1:1 v/v): δ = 25.9, 26.1, 29.3, 29.4, 29.6, 29.7, 30.9, 65.7, 68.5, 114.8, 122.6, 124.8, 129.1, 130.5, 146.9, 152.8, 161.8. MS (EI^-): m/z = 741.

3. Results and discussion

3.1. Isomerization of Azo-9P is highly affected by temperature and by the physical state of lipids

Trans-to-*cis* isomer conversion of Azo-9 P (Fig. 1A) can easily be tracked by UV/Vis spectroscopy as an increase in absorbance at 450 nm ($A_{450\ nm}$) and a decrease in absorbance at 350 nm ($A_{350\ nm}$). As detailed in Fig. 1B, the band at 350 nm corresponds to strong π—π* transitions in the trans-form, while these transitions are downshifted to 310 nm (hypsochromic) and weakened in the *cis*-state (Bandara and Burdette, 2012). The band at 450 nm is ascribed to n—π* transitions that are permitted to a higher extent (even though weak) in the *cis*-form than in the *trans*-form. This up-and-down pattern is illustrated in Fig. 1C, which shows changes in the absorbance spectra of Azo-9P upon exposure to light (365 nm) when incorporated in di-16:0 PC LUVs. Experiments were conducted at 50 °C, well above T_m of di-16:0 PC (T_m˜41 °C (Lewis et al., 1987)). At t = 0 s, the UV/Vis spectrum shows a strong absorption peak at 350 nm and a weak absorption peak at 450 nm. The position of the peak at 350 nm for the *trans*-isomer at t = 0 s indicates a homogeneous distribution of *trans*-azobenzene molecules along the lipid membrane and a low degree of chromophore clustering (Kuiper and Engberts, 2004). Upon prolonged exposure to light, A_{350nm} drops and A_{450nm} increases concomitantly. Additionally, the peak at 350 nm is downshifted to 310 nm as a consequence of the conversion of the azolipid to the *cis*-state (Kuiper and Engberts, 2004; Einaga et al., 1999). After approximately ˜30 min of light exposure no further changes in spectral properties are observed, indicating that the maximal extent of isomerization is reached.

The UV/Vis spectra of di-16:0 PC/Azo-9P mixtures were further investigated at 20 °C and at 30 °C, below T_m of di-16:0 PC (Lewis et al., 1987). For both temperatures the main absorption peak was found to be downshifted from 350 nm in the fluid phase to approximately 330 nm (Figure S1). This downshift may be ascribed to a high clustering degree between azobenzene moieties or to a close contact between chromophores, as a direct consequence of the tighter lipid packing in gel-phase membranes (Kuiper and Engberts, 2004). Calorimetric analyses confirmed that also in the presence of Azo-9P, di-16:0 PC lipids are in a gel-phase at 20 °C and at 30 °C, thus demonstrating only a mild disturbing effect of Azo-9P on the thermotropic properties of its surrounding lipids (Heimburg, 1998) (Figure S2).

Next, we quantified the rate and extent of the geometric conversion at different temperatures. The presence of two isosbestic points at 50 °C indicates that only two species are involved in the conversion reaction. *Xcis* values (defined as 1–$[A_{350}]_t/[A_{350}]_0$) are shown as function of the exposure time of the sample to the light beam (Fig. 2A). Data was fitted

Table 1
Isomerization rate constants (k) and isomerization degree values ($Xcis$) obtained from the isomerization of *trans*-Azo-9 P in different self-assemblies. All samples were prepared with 10 mol% Azo-9 P. Error bars represent the standard error of at least 2 independent experiments.

Self-assembly	Temperature (°C)	Composition	$Xcis_{max}$	k (min^{-1})
LUVs	20	di-16:0 PC	0.63 ± 0.06	0.09 ± 0.02
LUVs	30	di-16:0 PC	0.81 ± 0.01	0.11 ± 0.01
LUVs	50	di-16:0 PC	0.88 ± 0.02	0.23 ± 0.02
LUVs	50	di-16:0 PC/lyso PC (8:2 mol)	0.92 ± 0.02	0.69 ± 0.09
LUVs	50	di-16:0 PC/di-16:1 PC (8:2 mol)	0.83 ± 0.02	0.20 ± 0.01
SMA 2:1	50	di-16:0 PC	0.86 ± 0.02	0.75 ± 0.09
SMA 3:1	50	di-16:0 PC	0.89 ± 0.01	0.72 ± 0.05

to equation 2 (SI) to obtain the isomerization rate constants k of Azo-9 P (Table 1). It was found that *trans*-to-*cis* isomerization of Azo-9 P in di-16:0 PC fluid membranes (50 °C, T > T_m) takes place relatively fast with a rate constant k of approximately 0.23 min^{-1} (Fig. 2, Table 1). Slower isomerization rates were obtained when the isomerization was conducted at 30 °C and at 20 °C, with k values of 0.11 min^{-1} and 0.09 min^{-1} respectively. The difference in k values is mainly ascribed to temperature but may also be affected by the physical state of the lipids, with the tighter packing of the acyl chains in the gel phase causing a reduction of the isomerization rate. In principle, higher viscosity values may play a role in yielding slower photoisomerization rates. However this is unlikely to significantly contribute here, as no changes in isomerization rates were observed for azobenzene molecules in chloroform/polystyrene mixtures of increasing viscosity (Serra and Terentjev, 2008). Finally, it should be noted that isosbestic points obtained below the melting phase transition of the lipids (Figure S1) are somewhat less well defined than those obtained at 50 °C (Fig. 1). Nevertheless, also here a good quality of the fits is obtained (Fig. 2A) by assuming that geometric conversion followed first order kinetics (Whitten et al., 1971).

The results in Fig. 2A furthermore show a high extent of isomerization for *trans*-azobenzene molecules in fluid membranes, with $Xcis$ value of ˜0.92 after approximately ˜30 min of exposure to light. However, they exhibit lower $Xcis$ values of 0.63—0.81 when incorporated in gel-phase membranes (Table 1). The relatively low isomerization rates and low isomerization degree of *trans*-Azo-9P molecules in the gel phase are most likely a direct result from the high order parameters and tight packing of the lipids in this phase, since it was shown that bulky *cis*-Azo-9P molecules are difficult to accommodate in solid or highly ordered surfaces (Nakayama et al., 1997; Einaga et al., 1999).

3.2. The isomerization of Azo-9P is sensitive to the lipid composition of the host membrane

The effect of lipid packing on the rate and extent of isomerization of Azo-9P was further tested by using vesicle preparations of different composition. In particular, we used LUVs consisting of the host lipid di-16:0 PC and 20% (mol) of either di-16:1 PC or lyso PC as guest lipid. The azo group in Azo-9P is located at approximately the same depth in the lipid bilayer as the double bonds of di-16:1 PC (Δ9-cis), thus is directly exposed to the higher lateral pressure conditions promoted by the kink of the acyl chains. On the other hand, lower lateral pressure is expected in the hydrophobic part of the bilayer enriched in lyso PC due its relatively small hydrophobic volume. As shown in Fig. 2B and displayed in Table 1, the highest rate of isomerization was observed for LUVs supplemented with lyso PC lipids (k˜0.69 min^{-1}), while the rate of conversion is lowest for Azo-9 P incorporated in vesicles supplemented with di-16:1 PC (k˜0.20 min^{-1}). However, this only slightly affects the equilibrium, as the final extent of isomerization of Azo-9 P in LUVs with lyso-PC is not much larger than that in di-16:0 PC vesicles with or without di-16:1 PC (Table 1). Importantly, the results were likely not affected by the concentration of azolipids in the vesicles since this was kept rather constant as shown by the A350 value at t = 0 s (Table S1).

Overall, these data show that Azo-9P molecules are sensitive to the lipid composition of the membrane whereby a relatively large cross-sectional area of the acyl chains is likely to hamper the conversion of *trans*- into *cis*-Azo-9P isomers in the lipid environment.

3.3. Azo-9P molecules incorporated in SMA-nanodiscs isomerize fast and to a high extent

The sensitivity of isomerization rates and $Xcis$ values of Azo-9P to steric hindrance conditions was employed to elucidate to what extent SMA-bounded nanodiscs are able to accommodate an increase in area of enclosed molecules in the acyl chain region. It must be noted that azobenzene chromophores are covalently attached at C9, which is a position in which they are in close contact with the more ordered hydrophobic core of SMA-bounded nanodiscs (Orwick et al., 2012).

As shown in Fig. 2C, the isomerization rates of Azo-9P in di-16:0 PC bounded by either SMA 2:1 or SMA 3:1 (spectra are illustrated in Figure S3) both are extremely fast, with isomerization rates of 0.75 min^{-1} and 0.72 min^{-1} respectively. Furthermore, as shown in Fig. 2C and displayed in Table 1, azolipids in nanodiscs reach similar $Xcis$ values regardless of the polymer belt, with values of 0.86 for SMA 2:1 nanodiscs and 0.89 for SMA 3:1 nanodiscs. These results indicate that geometric changes are very easily accomodated in the presence of SMA, despite the increase in cross-sectional area in the center of the nanodiscs.

A complication in interpretation of the data arose from the following observation during preparation of the nanodiscs. Vesicles containing Azo-9P molecules were found to have a very poor solubilization efficiency as compared to the host phosphatidylcholine lipids, that were fully solubilized upon addition of SMA. We hypothesize that this was due to a high lateral pressure in the hydrophobic region due to the presence of the azo-group, in line with observed differences in solubilization efficiency in lipid mixtures, that were related to differences in lateral pressure profiles (Scheidelaar et al., 2015).The Azo-9P content in nanodiscs was estimated to be < 1 mol %. The concentration of azobenzene in nanodiscs was estimated from A_{350nm}, based on calibration with known concentrations of azobenzene in LUVs (Figure S4).

This has important consequences, because the extent of isomerization and the isomerization rates of Azo-9 P are affected by the order of the platform they are embedded in, thus probably will be also affected by the local abundance of azolipids due to the contribution of azobenzene groups to the lateral pressure profile in the hydrocarbon region of the membrane. This was supported by results obtained from LUVs with increasing amount of azobenzene-labeled lipids, where higher rates of isomerization were observed for samples with lower content of Azo-9P (Figure S5). Therefore, ideally one should compare data for nanodiscs and vesicles with the same Azo-9P content. Unfortunately, this was not possible, since we were not able to prepare nanodiscs with higher Azo-9P concentration and since vesicles in which we lowered the Azo-9P concentration to 1 mol % did not give sufficient sensitivity, due to an additional scattering contribution to the spectra. The low local abundance of Azo-9P in nanodiscs may explain why the particle size

distribution of nanodiscs is not shifted to bigger particle diameters after exposure to UV light (Figure S6). Nevertheless, we can safely conclude from our data that fast and efficient conversion does take place in nanodiscs.

4. Conclusion

We investigated the sensitivity of alkylated azobenzene molecules (Azo-9P) to changes in lipid phase behavior and in lipid composition of the membrane that they are embedded in. We have shown that the isomerization rate of Azo-9P is lowest when azolipids are present in highly ordered membranes and in membranes enriched with mono-unsaturated phospholipids. This is ascribed to the sensitivity of isomerization to the lipid packing properties in the hydrocarbon region of the membrane. Importantly, this study demonstrates that amphipathic SMA belts allow enclosed azobenzene labeled lipids in nanodiscs to fully isomerize in short periods of time, showing that SMA-bounded nanodiscs can easily accommodate an increase in geometric area in the acyl chain region. As such, the results support earlier findings that lipids in the nanodisc are less ordered than in vesicles or membranes (Jamshad et al., 2015; Orwick et al., 2012; Grethen et al., 2017; Dominguez Pardo et al., 2017; Domínguez Pardo et al., 2018). The observed dynamic character of SMA nanodiscs is also in line with the observations of collisional lipid exchange (Cuevas Arenas et al., 2017; Grethen et al., 2018; Domínguez Pardo et al., 2018) and polymer exchange (Schmidt, 2018) between nanodiscs. Finally, the observation that geometry changes of enclosed molecules are possible suggests that nanodiscs may provide a suitable bilayer environment for flexible proteins that undergo relatively large conformational changes during function.

Funding

This work was supported financially by NWO Chemical Sciences ECHO grant No. 711-013-005 (JJDP).

Conflicts of interest

The authors declare that there are no conflicts of interest.

Acknowledgements

Dr. E.J.Breukink (University of Utrecht) is acknowledged for helpful and critical discussions.

Appendix A. Supplementary data

Supplementary material related to this article can be found, in the online version, at doi:https://doi.org/10.1016/j.chemphyslip.2019.02.002.

References

Bandara, H.M.Dhammika, Burdette, Shawn C., 2012. Photoisomerization in different classes of azobenzene. Chem. Soc. Rev. 41 (5), 1809–1825. https://doi.org/10.1039/c1cs15179g. pág.

Beharry, Andrew A., Woolley, G. Andrew, 2011. Azobenzene photoswitches for biomolecules. Chem. Soc. Rev. 40 (8), 4422–4437. https://doi.org/10.1039/c1cs15023e. pág.

Cuevas Arenas, Rodrigo, Danielczak, Bartholomäus, Martel, Anne, Porcar, Lionel, Breyton, Cécile, Ebel, Christine, Keller, Sandro, 2017. Fast collisional lipid transfer among polymer-bounded nanodiscs. Sci. Rep. 7, 45875. https://doi.org/10.1038/srep45875. pág.

Dominguez Pardo, J.J., Dörr, J.M., Renne, M.F., Ould-Braham, T., Koorengevel, M.C., van Steenbergen, M.J., Killian, J.A., 2017. Thermotropic properties of phosphatidylcholine nanodiscs bounded by styrene-maleic acid copolymers. Chem. Phys. Lipids 208, 58–64. https://doi.org/10.1016/j.chemphyslip.2017.08.010. pág.

Domínguez Pardo, Juan J., Koorengevel, Martijn C., Uwugiaren, Naomi, Weijers, Jeroen, Kopf, Adrian H., Jahn, Helene, et al., 2018. Membrane solubilization by styrene-maleic acid copolymers. Delineating the role of polymer length. Biophys. J. 115 (1), 129–138. https://doi.org/10.1016/j.bpj.2018.05.032. pág.

Dörr, Jonas M., Koorengevel, Martijn C., Schäfer, Marre, Prokofyev, Alexander V., Scheidelaar, Stefan, Cruijsen, vander, Elwin, A.W., et al., 2014. Detergent-free isolation, characterization, and functional reconstitution of a tetrameric K+ channel. The power of native nanodiscs. Proc. Natl. Acad. Sci. 111 (52), 18607–18612 pág.

Dörr, Jonas M., Scheidelaar, Stefan, Koorengevel, Martijn C., Dominguez, Juan J., Schäfer, Marre, van Walree, CornelisA., Killian, J. Antoinette, 2016. The styrene-maleic acid copolymer: a versatile tool in membrane research. Eur. Biophys. J.: EBJ 45 (1), 3–21. https://doi.org/10.1007/s00249-015-1093-y. pág.

Einaga, Y., Sato, O., Iyoda, T., Fujishima, A., Hashimoto, K., 1999. Photofunctional vesicles containing prussian blue and azobenzene. J. Am. Chem. Soc. 121 (15), 3745–3750. https://doi.org/10.1021/ja982450l. pág.

Elbing, Mark, Błaszczyk, Alfred, Hänisch, Carstenvon, Mayor, Marcel, Ferri, Violetta, Grave, Christian, et al., 2008. Single component self-assembled monolayers of aromatic azo-biphenyl. Influence of the packing tightness on the SAM structure and light-induced molecular movements. Adv. Funct. Mater. 18 (19), 2972–2983. https://doi.org/10.1002/adfm.200800652. pág.

Esmaili, Mansoore, Overduin, Michael, 2017. Membrane biology visualized in nanometer-sized discs formed by styrene maleic acid polymers. Biochimica et biophysica acta. https://doi.org/10.1016/j.bbamem.2017.10.019.

Grethen, Anne, Oluwole, Abraham Olusegun, Danielczak, Bartholomäus, Vargas, Carolyn, Keller, Sandro, 2017. Thermodynamics of nanodisc formation mediated by styrene/maleic acid (2:1) copolymer. Sci. Rep. 7 (1), 11517. https://doi.org/10.1038/s41598-017-11616-z. pág.

Grethen, Anne, Glueck, David, Keller, Sandro, 2018. Role of coulombic repulsion in collisional lipid transfer among SMA(2:1)-bounded nanodiscs. J. Membr. Biol. 251 (3), 443–451. https://doi.org/10.1007/s00232-018-0024-0. pág.

Hazell, Gavin, Arnold, Thomas, Barker, Robert D., Clifton, Luke A., Steinke, Nina-Juliane, Tognoloni, Cecilia, Edler, Karen J., 2016. Evidence of lipid exchange in styrene maleic acid lipid particle (SMALP) nanodisc systems. Langmuir: ACS J. Surf. Colloids 32 (45), 11845–11853. https://doi.org/10.1021/acs.langmuir.6b02927. pág.

Heimburg, Thomas, 1998. Mechanical aspects of membrane thermodynamics. Estimation of the mechanical properties of lipid membranes close to the chain melting transition from calorimetry. Biochimica et Biophysica Acta (BBA) - Biomembranes 1415 (1), 147–162. https://doi.org/10.1016/S0005-2736(98)00189-8. pág.

Jamshad, Mohammed, Grimard, Vinciane, Idini, Ilaria, Knowles, Tim J., Dowle, Miriam R., Schofield, Naomi, et al., 2015. Structural analysis of a nanoparticle containing a lipid bilayer used for detergent-free extraction of membrane proteins. Nano Res. 8 (3), 774–789. https://doi.org/10.1007/s12274-014-0560-6. pág.

Kuiper, Johanna M., Engberts, Jan B.F.N., 2004. H-aggregation of azobenzene-substituted amphiphiles in vesicular membranes. Langmuir: ACS J. Surf. Colloids 20 (4), 1152–1160. https://doi.org/10.1021/la0358724. pág.

Kuiper, Johanna M., Hulst, Ron, Engberts, Jan B.F.N., 2003. A selective and mild synthetic route to dialkyl phosphates. Synthesis 2003 (05), 695–698 pág.

Lewis, Ruthven N.A.H., Mak, Nanette, McElhaney, Ronald N., 1987. A differential scanning calorimetric study of the thermotropic phase behavior of model membranes composed of phosphatidylcholines containing linear saturated fatty acyl chains. Biochemistry 26 (19), 6118–6126 pág.

Nakayama, Keisuke, Jiang, Lei, Iyoda, Tomokazu, Hashimoto, Kazuhito, Fujishima, Akira, 1997. Photo-induced structural transformation on the surface of azobenzene crystals. Jpn. J. Appl. Phys. 36 (6S), 3898. pág. Disponible en línea en. http://stacks.iop.org/1347-4065/36/i=6S/a=3898.

Orwick, Marcella C., Judge, Peter J., Procek, Jan, Lindholm, Ljubica, Graziadei, Andrea, Engel, Andreas, et al., 2012. Detergent-free formation and physicochemical characterization of nanosized lipid-polymer complexes: lipodisq. Angew. Chem. (Int. ed. English) 51 (19), 4653–4657. https://doi.org/10.1002/anie.201201355. pág.

Prabudiansyah, Irfan, Kusters, Ilja, Caforio, Antonella, Driessen, Arnold J.M., 2015. Characterization of the annular lipid shell of the Sec translocon. Biochimica et biophysica acta 1848 (10 Pt A), 2050–2056. https://doi.org/10.1016/j.bbamem.2015.06.024. pág.

Rouser, George, Fleischer, Sidney, Yamamoto, Akira, 1970. Two dimensional thin layer chromatographic separation of polar lipids and determination of phospholipids by phosphorus analysis of spots. Lipids 5 (5), 494–496 pág.

Scheidelaar, Stefan, Koorengevel, Martijn C., Pardo, Juan Dominguez, Meeldijk, Johannes D., Breukink, Eefjan, Killian, J. Antoinette, 2015. Molecular model for the solubilization of membranes into nanodisks by styrene maleic acid copolymers. Biophys. J. 108 (2), 279–290. https://doi.org/10.1016/j.bpj.2014.11.3464. pág.

Schmidt, Victoria, Sturgis, James N., 2018. Modifying styrene-maleic acid co-polymer for studying lipid nanodiscs. Biochimica et biophysica acta. Biomembranes 1860 (3), 777–783. https://doi.org/10.1016/j.bbamem.2017.12.012. pág.

Serra, Francesca, Terentjev, Eugene M., 2008. Effects of Solvent Viscosity and Polarity on the Isomerization of Azobenzene. Macromolecules 41 (3), 981–986. https://doi.org/10.1021/ma702033e. pág.

Stroud, Zoe, Hall, Stephen C.L., Dafforn, Tim R., 2018. Purification of membrane proteins free from conventional detergents. SMA, new polymers, new opportunities and new insights. Methods (San Diego, Calif.) 147, 106–117. https://doi.org/10.1016/j.ymeth.2018.03.011. pág.

Sun, Chang, Benlekbir, Samir, Venkatakrishnan, Padmaja, Wang, Yuhang, Hong, Sangjin, Hosler, Jonathan, et al., 2018. Structure of the alternative complex III in a supercomplex with cytochrome oxidase. Nature 557 (7703), 123–126. https://doi.org/10.1038/s41586-018-0061-y. pág.

Swainsbury, David J.K., Scheidelaar, Stefan, van Grondelle, Rienk, Killian, J. Antoinette, Jones, Michael R., 2014. Bacterial reaction centers purified with styrene maleic acid copolymer retain native membrane functional properties and display enhanced stability. Angew. Chem. (International ed. in English) 53 (44), 11803–11807 pág.

Whitten, David G., Wildes, Peter D., Pacifici, J.G., Irick, Gether, 1971. Solvent and substituent on the thermal isomerization of substituted azobenzenes. Flash spectroscopic study. J. Am. Chem. Soc. 93 (8), 2004–2008. https://doi.org/10.1021/ja00737a027. pág.

Xue, Minmin, Cheng, Lisheng, Faustino, Ignacio, Guo, Wanlin, Marrink, Siewert J., 2018. Molecular Mechanism of Lipid Nanodisk Formation by Styrene-Maleic Acid Copolymers. Biophy. J. 115 (3), 494–502. https://doi.org/10.1016/j.bpj.2018.06.018. pág.